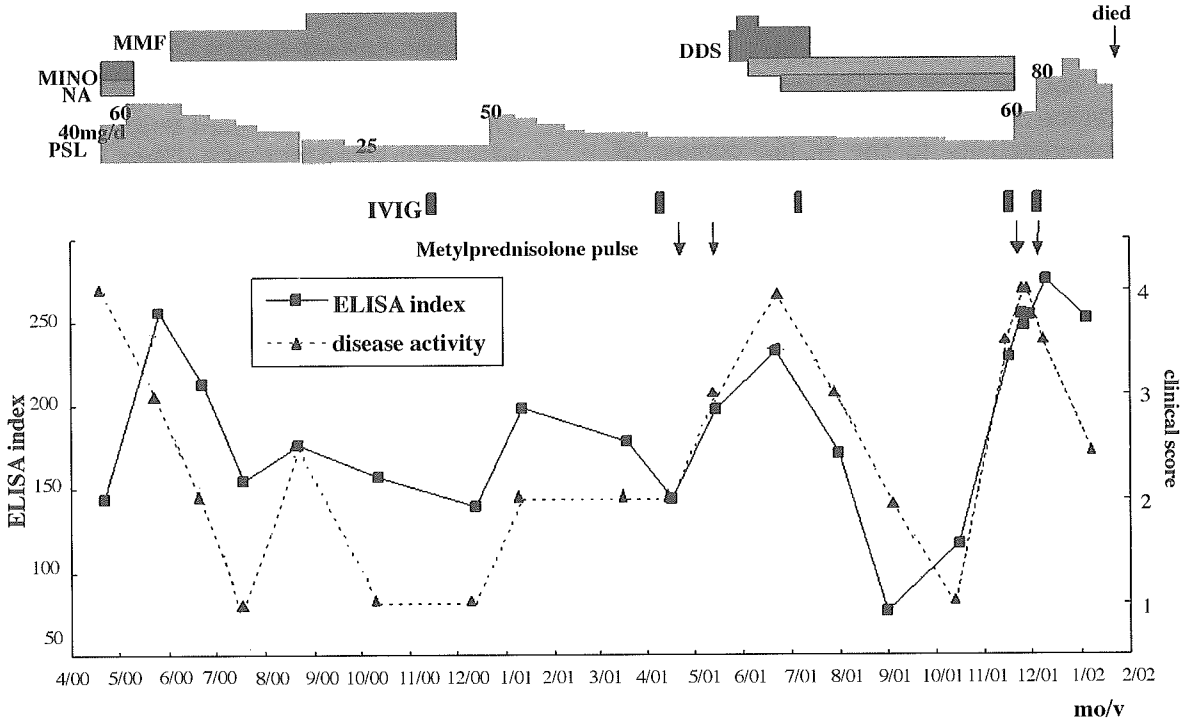

Fig. 2 Correlation of clinical course and ELISA indices in the severely affected BP patient: the mean ELISA index of this patient was much higher than those of other BP patients in the present study. Throughout the disease course, ELISA indices were well correlated with the disease activity, even in this extraordinarily severe case, that was resistant to treatment. DDS, diamino-diphenyl sulfone; IVIG, intravenous immunoglobulin G; MINO, minocycline; MMF, mycophenolate mofetil; NA, nicotinamide; PSL, predonisolone.

4. Discussion

BP180 ELISA kit specifically measures the titres of autoantibodies binding to the NC16a domain, the major pathogenic epitope in the extracellular domain of BPAG2. In this report, we studied typical BP patients' sera using a commercially available NC16A ELISA kit and revealed that 11 out of 14 patients who showed complete disease remission demonstrated significant reduction in the ELISA index after treatment (Fig. 1a). The remaining 3 out of 14 patients' (Fig. 1a; patients 4, 5 and 9) ELISA indices were under the cut-off value even before treatment. In previous studies, the majority of BP patients reacted with BP180 NC16A domain and the recombinant protein of this region was thought to be more suitable than epidermal extracts as an antigen source for detecting circulating anti-BP180 autoantibodies [1,3,7]. Hata et al. [4] reported that 84.4% BP sera showed positive reactivity against bacterial recombinant peptide of the entire extracellular domain of BP180 (rBP180EC) by immunoblot analysis, and that 67.5% BP sera were positive for rBP180EC by ELISA. They also demonstrated the reactivity of BP sera against rBP180EC by ELISA was completely abolished or significantly reduced by immunocompetition with bacterial recombinant peptide of the NC16A domain of BP180 in most of the sera, while the reactivity was not altered in the other sera [4]. Later, Kobayashi et al. [7] reported that the sensitivity of BP ELISA using bacterial recombinant NC16a protein in BP patients was 84.4%. These results suggest that, in some BP patients, sera might be reactive against minor epitopes other than NC16A domain. This agrees with the present results that 3 out of 14 BP patients examined were BP180 ELISA-negative and that these sera might be reactive against other pathogenic epitopes in these patients.

We also demonstrated that IIF titres were reduced after successful treatment in 11 of 14 patients (Fig. 1b), whereas 2 patients revealed increased IIF titres after remission (Fig. 1b; patients 4 and 9). These patients also had negative ELISA indices, suggesting IIF might not be useful for ELISA-negative patients. It is reported that the titres of circulating autoantibodies detected by IIF do not always correlate with the disease activity, as IIF detects not only anti-BPAG2 autoantibodies but also autoantibodies against BPAG1, the intracellular molecule that would not directly contribute to the pathogenesis of BP [9–12]. Moreover, it is reported that IIF titres of BP patients' sera mainly reflect the amount of circulating anti-BPAG1 anti-

bodies rather than of the pathogenic anti-BPAG2 antibodies [12]. From these findings, it is suggested that IIF is not the best way to measure disease activity. On the other hand, Amo et al. [6] reported that immunoreactivity to the NC16A domain of BP180 examined by NC16A-ELISA was clearly correlated with the clinical course of the BP patients. In addition, Kobayashi et al. [7] described that, in seven BP patients, NC16a ELISA socres tended to fluctuate in parallel with the disease during the time course and reflected the disease activity much better than IIF. Hofmann et al. [13] also showed that levels of IgG against NC16A domain and collagenous Col15 domain of BP180 reflected disease severity indicating that autoantibodies against the NH_2-terminus are critical in the pathogenesis of BP. From our present results, BP180 NC16A ELISA is thought to be useful in evaluating disease activity in the cases showing positive BP180 NC16A ELISA at the initial examination, although it has limitations and cannot be used if the patient's pathogenic epitope is located outside the NC16A domain.

We experienced an unusual, severely affected BP patient in which, unfortunately, we could not control the disease activity in spite of various treatments. Interestingly, in this severe case, the ELISA indices precisely correlated with the disease activity throughout the 21-month follow-up period in the patient (Fig. 2). The patient's mean ELISA indices were much higher than those of the 10 other untreated BP patients. The high ELISA indices in this patient probably imply an extremely high level of pathogenic autoantibodies to NC16A domain of BPAG2 that resulted in the poor prognosis.

In conclusion, the ELISA index measured by the BP180 ELISA kit that specifically recognizes the NC16A domain of BPAG2 correlates well with the disease activity. This commercially available kit is a useful tool to evaluate the disease activity and to assess the effectiveness of the treatment of BP.

References

[1] Giudice GJ, Emery DJ, Zelickson BD, Anhalt GJ, Liu Z, Diaz LA. Bullous pemphigoid and herpes gestationis autoantibodies recognize a common non-collagenous site on the BP180 ectodomain. J Immunol 1993;151:5742–50.

[2] Zillikens D, Mascaro JM, Rose PA, Liu Z, Ewing SM, Caux F, et al. A highly sensitive enzyme-linked immunosorbent assay for the detection of circulating anti-BP180 autoantibodies in patients with bullous pemphigoid. J Invest Dermatol 1997; 109:679–83.

[3] Nakatani C, Muramatsu T, Shirai T. Immunoreactivity of bullous pemphigoid (BP) autoantibodies against the NC16A and C-terminal domains of the 180 kDa BP antigen (BP180): immunoblot analysis and enzyme-linked immunosorbent assay using BP180 recombinant proteins. Br J Dermatol 1998;139:365–70.

[4] Hata Y, Fujii Y, Tsunoda K, Amagai M. Production of the entire extracellular domain of BP180 (type XVII collagen) by baculovirus expression. J Dermatol Sci 2000;23:183–90.

[5] Schmidt E, Obe K, Brocher EB, Zillikens D. Serum levels of autoantibodies to BP180 correlate with diesase activity in patients with bullous pemphigoid. Arch Dermatol 2000;136: 174–8.

[6] Amo Y, Ohkawa T, Tatsuta M, Hamada Y, Fujimura T, Katsuoka K, et al. Clinical significance of enzyme-linked immunosorbent assay for the detection of circulating anti-BP180 autoantibodies in patients with bullous pemphigoid. J Dermatol Sci 2001;26:14–8.

[7] Kobayashi M, Amagai M, Kuroda-Kinoshita K, Hashimoto T, Shirakata Y, Hashimoto K, et al. BP180 ELISA using bacterial recombinant NC16a protein as a diagnostic and monitoring tool for bullous pemphigoid. J Deramtol Sci 2002;30: 224–32.

[8] Beutner EH, Jordon RE, Chorzelski TP. The immunopathology of pemphigus and bullous pemphigoid. J Invest Dermatol 1968;51:63–80.

[9] Ishiko A, Shimizu H, Kikuchi A, Ebihara T, Hashimoto T, Nishikawa T. Human autoantibodies against the 230-kD bullous pemphigoid antigen (BPAG1) bind only to the intracellular domain of the hemidesmosome, whereas those against the 180-kD bullous pemphigoid antigen (BPAG2) bind along the plasma membrane of the hemidesmosome in normal human and swine skin. J Clin Invest 1993;91: 1608–15.

[10] Ahmed AR, Maize JC, Provost TT. Bullous pemphigoid: clinical and immunologic follow-up after successful therapy. Arch Dermatol 1977;113:1043–6.

[11] Zillikens D, Ambach A, Schuessler M, Dummer R, Hartmann AA, Burg G. The interleukin-2 receptor in lesions and serum of bullous pemphigoid. Arch Dermatol Res 1992;284:141–5.

[12] Pas HH, de Jong MC, Jonkman MF, Heeres K, Slijper-Pal IJ, van der Meer JB. Bulllous pemphigoid: serum antibody titre and antigen specificity. Exp Dermatol 1995;4:372–6.

[13] Hofmann S, Thoma-Uszynski S, Hunziker T, Bernard P, Koebnick C, Stauber A, et al. Severity and phenotype of bullous pemphigoid relate to autoantibody profile against the NH2- and COOH-terminal regions of the BP180 ectodomain. J Invest Dermatol 2002;119:1065–73.

Available online at www.sciencedirect.com
SCIENCE DIRECT®

Zinc dental fillings and palmoplantar pustulosis

Teruki Yanagi, Tadamichi Shimizu, Riichiro Abe and Hiroshi Shimizu

Lancet 2005; 366: 1050

Department of Dermatology (T Yanagi MD, T Shimizu MD, R Abe MD, H Shimizu MD), **Hokkaido University Graduate School of Medicine, N15W7, Kita-ku, Sapporo 060-8638, Japan**

Correspondence to: Dr Teruki Yanagi
yanagi@med.hokudai.ac.jp

In January, 2005, a 59-year-old Japanese woman was referred to our hospital with a 5-week history of inflammatory skin lesions on her palms and soles. Physical examination revealed multiple pustules, vesicles, and scaly erythema disseminated over her palms and soles; clinically, the signs were typical of palmoplantar pustulosis (PPP) (figure). Laboratory data and complete blood counts were within normal limits. She had no tonsillitis and a pharyngeal culture test was negative. Detailed medical history revealed that the patient had received extensive treatment for dental caries with dental metal restorations for five teeth 1 year earlier. We suspected a possible relation between the PPP and dental metal allergy. To see whether there was any metal allergy, we did patch testing on her forearm with the metal standard patch test series (Torii Pharmaceutical Co, Ltd, Tokyo, Japan), including aluminium chloride, chromium sulphate, cobalt chloride, copper sulphate, ferric chloride, gold chloride, indium trichloride, iridium tetrachloride, manganese chloride, mercury bichloride, nickel sulphate, platinum chloride, palladium chloride, potassium dichloride, stannous chloride, silver bromide, and zinc chloride. After 48 h there was a pronounced positive reaction with zinc; all other tests were negative. Severe exudative erythema with multiple pustules, clinically similar to PPP, appeared in the patch test area resulting from zinc chloride 2% petrolatum (figure, inset). Skin biopsy of the test site showed sterile, intraepidermal pustules, pathologically identical to PPP. Furthermore, drug lymphocyte stimulating tests (DLST) revealed a very strong reaction to zinc sulphate with stimulating index 1880% (normal <180%). Analysis of her dental filling showed that it contained gold, indium, silver, palladium, copper, tin, and zinc.

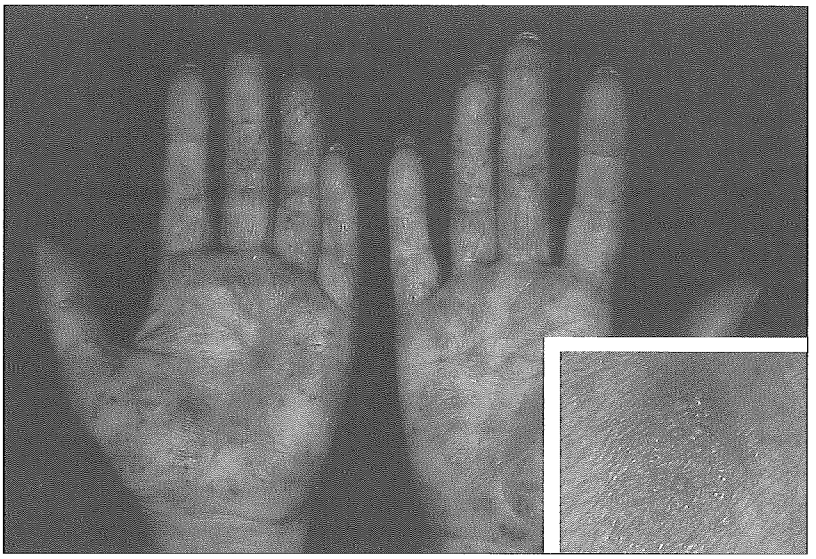

Figure: **Palmoplantar pustulosis showing pustules, vesicles, and scaly erythema**
Inset: pustule formation, clinically equivalent to PPP, was observed over the zinc chloride patch test area (after 48 h).

On the basis of clinical history, positive patch test with characteristic histology, and positive DLST index, we concluded that the patient's PPP was induced by zinc allergy. Therefore, all her dental fillings were completely removed and changed to a zinc-free compound. Although no oral or topical medication was given, the patient's PPP showed an improvement soon after the removal of the fillings, and complete cure was achieved in only 4 weeks. When last seen in July, 2005, the patient was well and there has been no sign of recurrence.

PPP is a chronic skin disease characterised by sterile intraepidermal pustules associated with erythematous scaling on the palms and soles.[1] Although the cause of PPP is not completely known, association with thyroid disease, smoking, and focal infections, such as tonsillitis, has been suggested.[1,2] Recently, metal allergy associated with PPP, including nickel, iron, and cobalt, has been reported.[3] Here we report zinc-allergy-induced PPP in which histologically identical pustules were produced by zinc patch test, and a complete remission was subsequently achieved by removal of zinc dental restorations. The relation between PPP and metal allergy has been reported in the Japanese population, but this has not been widely recognised elsewhere.[3,4]

References

1 Eriksson MO, Hagforsen E, Lundin IP, Michaelsson G. Palmoplantar pustulosis: a clinical and immunohistological study. *Br J Dermatol* 1998; **138**: 390–98.

2 Akiyama T, Seishima M, Watanabe H, Nakatani A, Mori S, Kitajima Y. The relationships of onset and exacerbation of pustulosis palmaris et plantaris to smoking and focal infections. *J Dermatol* 1995; **22**: 930–34.

3 Nakamura K, Imakado S, Takizawa M, et al. Exacerbation of pustulosis palmaris et plantaris after topical application of metals accompanied by elevated levels of leukotriene B4 in pustules. *J Am Acad Dermatol* 2000; **42**: 1021–25.

4 Nakayama H, Nogi N, Kasahara N, Matsuo S. Allergen control. An indispensable treatment for allergic contact dermatitis. *Dermatol Clin* 1990; **8**: 197–204.

American Journal of Pathology, Vol. 167, No. 6, December 2005
Copyright © American Society for Investigative Pathology

Cell Injury, Repair, Aging and Apoptosis

Tissue Regeneration Using Macrophage Migration Inhibitory Factor-Impregnated Gelatin Microbeads in Cutaneous Wounds

Yunan Zhao,* Tadamichi Shimizu,* Jun Nishihira,† Yoshikazu Koyama,‡ Toshihiro Kushibiki,§ Ayumi Honda,* Hirokazu Watanabe,* Riichiro Abe,* Yasuhiko Tabata,§ and Hiroshi Shimizu*

From the Departments of Dermatology and Biochemistry,† Hokkaido University Graduate School of Medicine, Sapporo; Genetic Laboratory,‡ Sapporo; and the Institute for Frontier Medical Science,§ Kyoto University, Kyoto, Japan*

Migration inhibitory factor (MIF) responds to tissue damage and regulates inflammatory and immunological processes. To elucidate the function of MIF in cutaneous wound healing, we analyzed MIF knockout (KO) mice. After the excision of wounds from the dorsal skin of MIF KO and wild-type (WT) mice, healing was significantly delayed in MIF KO mice compared to WT mice. Lipopolysaccharide treatment significantly increased [^{3}H]thymidine uptake in WT mouse fibroblasts compared to MIF KO mouse fibroblasts. Furthermore, there was a significant reduction in fibroblast and keratinocyte migration observed in MIF KO mice after 1-oleoyl-2-lysophosphatidic acid treatment. We subsequently examined whether MIF-impregnated gelatin slow-release microbeads could accelerate skin wound healing. Injection of more than 1.5 μg/500 μl of MIF-impregnated gelatin microbeads around a wound edge accelerated wound healing compared to a single MIF injection without the use of microbeads. MIF-impregnated gelatin microbeads also accelerated skin wound healing in C57BL/6 mice and diabetic *db/db* mice. Furthermore, incorporating MIF-impregnated gelatin microbeads into an artificial dermis implanted into MIF KO mice accelerated procollagen production and capillary formation. These findings suggest that MIF is crucial in accelerating cutaneous wound healing and that MIF-impregnated gelatin microbeads represent a promising treatment to facilitate skin wound healing. *(Am J Pathol 2005, 167:1519–1529)*

The process of wound healing is complex, comprising inflammation, granulation tissue formation, and remodeling of tissues. Several growth factors/cytokines play important roles in tissue repair and enhance the wound-healing process. The expression of the proinflammatory cytokines, interleukin (IL)-1α, IL-1β, IL-6, and tumor necrosis factor-α during wound repair are up-regulated during the inflammatory wound-healing phase.[1] Polymorphonuclear leukocytes and macrophages were shown to be major sources of these cytokines, but expression was also observed in some resident cell types.[2,3] The coordinated up-regulation of these cytokines is likely to be important in normal tissue repair because the expression of these genes is markedly reduced after wounding in both healing-impaired glucocorticoid-treated mice and genetically diabetic *db/db* mice.[4]

The cytokine macrophage migration inhibitory factor (MIF) was first identified more than 30 years ago as a T-cell-derived factor that inhibits the random migration of macrophages.[5,6] MIF was recently re-evaluated as a proinflammatory cytokine and has been shown to be a pituitary-derived hormone that potentiates endotoxemia.[7–9] Subsequent work showed that T cells and macrophages secrete MIF in response to glucocorticoids as well as on activation by various proinflammatory stimuli.[8] This protein is ubiquitously expressed in various organs, including the skin, brain, and kidney.[10] Recently, it was reported that MIF mRNA expression was up-regulated during peripheral nerve regeneration.[11] We demonstrated that MIF is an immunoregulatory protein in the pathophysiology of skin disease.[12,13] Furthermore, ultraviolet B exposure *in vivo* increased the production of MIF,

Supported by the Ministry of Education, Science, and Culture of Japan (grants-in-aid for research no.11670813 and no. 13357008) and the Mitsui Sumitomo Insurance Welfare Foundation.

Y.Z. and T.S. contributed equally to this work.

Accepted for publication August 4, 2005.

Current address of T.S.: Department of Dermatology, Toyama University School of Medicine, Toyama, Japan.

Address reprint requests to Hiroshi Shimizu, Department of Dermatology, Hokkaido University Graduate School of Medicine, Sapporo 060-8638, Japan. E-mail: shimizu@med.hokudai.ac.jp.

suggesting its involvement in tissue injury.[14] To date, MIF responses to stimuli such as wounds and infections have been observed, and these responses are considered to contribute to the regulation of inflammatory and immunological responses to tissue damage.[15,16] Based on the previous findings, it is probable that MIF is closely associated with the wound-healing processes.

In the skin, MIF is expressed in the epidermis, particularly within the basal keratinocyte layer.[17] We have previously demonstrated that an increase in MIF expression during the cutaneous wounding process and MIF production in wounded fibroblasts could be initiated by lipopolysaccharide (LPS) stimulation.[15] MIF also had a chemotactic effect on keratinocytes and the administration of anti-MIF antibodies induced a delay in mouse wound healing.[15] Moreover, thrombin and factor Xa induced MIF expression in human dermal microvascular endothelial cells, suggesting that MIF contributes to the inflammatory phase of the wound-healing process.[18] However, a recent report indicated that MIF-deficient wound healing was not significantly different compared with wild-type (WT) mice.[19] In the present study, to further elucidate the function of MIF during the wound-healing process, we studied the cutaneous wounding process using MIF knockout (KO) mice that were recently established. We assessed the effects of adding exogenous MIF-impregnated gelatin microbeads providing a controlled release of MIF during the experimental time course. Our observations clearly indicated that MIF is crucial for cutaneous wound healing and MIF-impregnated gelatin microbeads show every indication of becoming a possible therapy for increasing the rate of wound healing.

Materials and Methods

Materials

The following materials were obtained from commercial sources. Rat monoclonal antibody against anti-mouse CD31 was purchased (PharMingen, San Diego, CA); anti-β-actin antibodies were purchased from Sigma-Aldrich Co. (St. Louis, MO); Dulbecco's modified eagle medium (DMEM), keratinocyte/serum-free medium containing bovine pituitary extract, and recombinant epidermal growth factor were from Invitrogen (Groningen, The Netherlands); the Isogen RNA extraction kit was from Nippon Gene (Toyama, Japan); Tissue-Tek OCT compound was from Miles Scientific (Elkhart, Naperville, IL); 1-oleoyl-2-lysophosphatidic acid (LPA) and LPS were from Sigma-Aldrich Co.; [^{3}H]thymidine (35 Ci/mmol) from Amersham Biosciences Corp. (Piscataway, NJ); terminal dUTP nick-end labeling (TUNEL) assay kit from Takara Bio Inc. (Shiga, Japan). Rho family GTPase activity was assessed using a commercially available kit (Cytoskeleton, Inc., Denver, Co) and transwell chambers with 8-μm pore-sized membranes from Kurabo (Osaka, Japan). Recombinant rat MIF was expressed in *Escherichia coli* BL21/DE3 (Novagen, Madison, WI) and was purified as described previously.[18] The purified MIF contained less than 1 pg of endotoxin per μg of protein, as determined by chromogenic Limulus amoebocyte assay (BioWhittaker, Walkersville, MD). The artificial dermis (Pelnac; Gunze Co., Kyoto, Japan) used in the present study was composed of an outer silicone layer and inner collagen sponge layer. All other chemicals were of reagent grade or higher.

Mice

Using targeted disruption of the MIF gene, a novel mouse strain (bred on a C57BL/6 background) deficient in MIF was established.[18] We repeated backcrossing the BALB/c background mice, originally established by Honma and colleagues,[20] with C57BL/6 mice, and used 10th generation mice that were genetically pure. C57BL/6 mice and *db/db* mice, a rodent model of type 2 diabetes were purchased from Japan Clea (Shizuoka, Japan) and maintained under specific pathogen-free conditions. All animal procedures were conducted according to the guidelines set out by the Hokkaido University Institutional Animal Care and Use Committee under an approved protocol. All experiments were performed on 8- to 10-week-old female adult mice.

Assessment of Wound Healing

For wound-healing experiments, we assessed the rate of wound healing.[21] MIF KO and WT mice were anesthetized with 40 mg/kg of sodium pentobarbital solution (intraperitoneally) and their dorsal hair clipped. Four full-thickness, round skin wounds (5-mm-diameter round punch biopsies) were prepared using a disposable skin biopsy punch (Maruho Co., Ltd., Osaka, Japan) (on day 0). The four wounds were separated 1 cm from each other. Then the wound diameter was measured every day until healing was completed. We examined the appearance of the skin wound until the full epithelial surface in all four wounds was restored in each mouse. In some experiments, to pathologically evaluate the skin regeneration state, MIF KO and WT mice samples were obtained, fixed, and processed for paraffin embedding and with hematoxylin and eosin staining at 5 days after wounding.

Cell Culture

Skin was obtained from the dorsal surface of newborn MIF KO mice and WT mice. The back of the mouse skin was excised and fibroblast cultures were obtained using a standard explant technique as previously described.[22] Briefly, the skin was cut into between 3- to 5-mm pieces and placed onto a large Petri dish with the subcutaneous side down and the tissue was incubated for 1 week in a humidified atmosphere of 5% CO_2 at 37°C. Once a sufficient number of fibroblasts had migrated out from the skin sections, pieces of skin were removed and the cells passaged by trypsin digestion in the same manner as wound-harvested fibroblasts. Fibroblasts were grown in DMEM containing 10% fetal calf serum and 1% penicillin/streptomycin. For keratinocyte isolation the epidermis was separated from dermis using dispase, and the ker-

atinocytes cultured in keratinocyte/serum-free medium containing bovine pituitary extract (30 μg/ml), recombinant epidermal growth factor (0.1 ng/ml), and 0.02 mmol/L $CaCl_2$. The fibroblast and keratinocytes cells (passage number 3) were used for the experiments.

Fibroblast Proliferation Assay

Skin was originally isolated from the backs of baby mice derived from both MIF KO and WT mice, and maintained in DMEM (Invitrogen) supplemented with 10% fetal calf serum and 0.01% penicillin/streptomycin. Mouse fibroblasts were seeded in 96-well plates at densities of 1000 cells/well in DMEM/10% fetal calf serum. The culture medium was changed to DMEM/0.4% fetal calf serum (subsequently designated as basal medium for these studies) after 12 hours. After 24 hours, LPS was added to give a range of final concentrations from 0 to 1.0 μg/ml. Cells were further incubated for 3 days and 1 μCi of [^{3}H]thymidine, was introduced into each well. After 24 hours, the medium was removed and cells were washed twice each with PBS and ice-cold trichloroacetic acid (5%). The precipitated material was dissolved in 0.3 N NaOH-solution and incorporated [^{3}H]thymidine was determined in a scintillation counter.

Fibroblast Apoptosis Assay

The number of apoptotic cells was determined by the TUNEL assay using a commercial kit. Fibroblasts from both MIF KO and WT mice were cultured and stimulated by LPS (1.0 μg/ml) in eight-well plates (5×10^3 cells per well) for 24 hours. The numbers of TUNEL-positive cells per 100 cells in a field were counted under the microscope.

Collagen Gel Contraction Assays

Collagen gel contraction assays were performed as described by Basu and colleagues.[23] Briefly, six-well tissue culture plates were made with a nonadhesive coating of 1% agarose. One volume of a solution of 3 mg/ml of bovine type I collagen was combined with 1/6 vol of 7× DMEM and sufficient 1× DMEM added to yield a final collagen concentration of 0.75 mg/ml. A suspension of fibroblasts from both MIF KO and WT mice at 2×10^6 cell/ml in DMEM was added to 9 vol of the type I collagen solution, and fetal bovine serum added to provide a concentration of 2% fetal bovine serum in the final solution. The resulting cell suspension was dispensed into agarose-coated wells (2 ml/well) and polymerized for 2 hours at 37°C. DMEM (2 ml) with 2% fetal bovine serum was subsequently added to the wells and the gels were gently detached from the walls to float the collagen disks. The collagen/cell mixtures were incubated in humidified air at 37°C and gel contraction monitored throughout 48 hours. The assay was performed six times. The area of gels was calculated from the final average diameter of the experiments and expressed as a percentage of the initial collagen gel area.

Migration Assay

The fibroblast migration assay was examined by the method of Mannino and colleagues.[24] Briefly, after the initial plating of fibroblasts from MIF KO and WT mice for 48 hours on culture dishes, cells were then scraped off using a yellow pipette tip. LPA (0 and 10 μmol/L) in DMEM containing 0.2% fatty acid-free bovine serum albumin was added to the culture dishes. Subsequently at 6 and 12 hours, the numbers of cells that had moved from the baseline were counted at high (×40) magnification. In each experiment, the numbers of cells that had migrated from four high-power fields from each well were counted. The Boyden chamber cell migration assay was also performed for fibroblast and keratinocyte migration using transwell chambers with 8-μm pore-sized membranes. The chambers were inserted into 24-well culture plates containing 0 and 10 μmol/L of LPA in DMEM containing 0.2% fatty acid-free bovine serum albumin or keratinocyte/serum-free medium. The cells (1×10^4) were loaded into the upper volume of Boyden chambers. Subsequently at 6 hours, nonmigrating cells were removed with a cotton swab, and cells were fixed in methanol for 15 minutes and stained with crystal violet. The migrating activity was quantified by blind counting of the migrating cells on the lower surface of the membrane of 10 fields per chamber using a 100× objective lens microscope.

RhoGTPase Activation Assay

The effect of LPA on activated GTP-RhoA, GTP-Cdc42, and GTP-Rac1 in fibroblasts was assessed using a commercially available pull-down assay. This assay utilizes the Rho-binding domain from the effector protein Rhotekin as a probe to specifically isolate the active forms of RhoA, Cdc42, and Rac1, the activity was detected by the method recently described by Benard and colleagues.[25] Cells (2×10^6) were seeded in 10-cm dishes. After cells were stimulated by LPA (10 μmol/L) in a time-dependent manner, beads were washed, eluted in sample buffer, and analyzed by Western blotting using monoclonal antibody against anti-RhoA (1:500) or polyclonal antibodies against Rac1 and Cdc42 (1:500).

Gelatin Hydrogels Incorporating MIF

A biodegradable hydrogel matrix (in the form of gelatin microbeads) was prepared by a chemical cross-linking of acidic or basic gelatin that was gradually enzymatically degraded in the body throughout time. The degradation is controllable by changing the extent of crosslinking, which, in turn, produces different hydrogel types with different water contents. The time course of the MIF protein release correlates well with the rate of hydrogel degradation.[26] Recombinant rat MIF (30 μg/20 μl) was dissolved in 2 mg of acidic gelatin microbeads (isoelectric point = 5.0) and was centrifuged, then the pellet stored for 30 minutes at room temperature. To examine whether recombinant rat MIF was actually impregnated into the gelatin microbeads, the putative MIF-impregnated gela-

tin microbeads were dispersed in 6 ml of phosphate-buffered saline (PBS) and stored for 48 hours. The MIF content in the PBS (the supernatant after the centrifugation) was then determined by MIF enzyme-linked immunosorbent assay (ELISA). As a control, free MIF (30 μg/20 μl) was dissolved in 6 ml of PBS. After it was confirmed that MIF was impregnated in the gelatin microbeads, we used the MIF-impregnated gelatin microbeads in the following protocols.

Effect of MIF-Containing Hydrogel Microbeads in Mice

To examine the effect of MIF-containing hydrogel microbeads in MIF KO mice, four full-thickness, round skin wounds (5-mm-diameter round punch biopsies) were prepared using a disposable skin biopsy punch on day 0 as described above. On day 1, MIF-impregnated gelatin microbeads (0 to 6 μg/500 μl) were inserted around the wound edge (n = 10 in each group). As a control, 3 μg/500 μl of MIF in PBS without hydrogel microbeads was directly injected into the wound edges (n = 10). Wound-healing assessment was performed as described above. Similarly, C57BL/6 mice and *db/db* mice were used to assess the wound healing with MIF-containing hydrogel microbeads. In some experiments, 3 μg/500 μl of MIF in hydrogel microbeads or 3 μg/500 μl of MIF in PBS without hydrogel microbeads were injected into the backs of MIF KO mice on day 0. On day 10, 5-mm-diameter skin biopsies were obtained and subjected to Western blot analysis.[27,28]

Implantation of Artificial Dermis

Full-thickness (dermis and epidermis) square skin wounds (10 mm in diameter) were prepared on the backs of MIF KO mice. MIF-impregnated gelatin microbeads (150 μg/100 μl) were injected into an artificial dermal scaffold (10 × 10 mm) (Pelnac, Gunze Co.). We then implanted an artificial dermal scaffold containing the MIF-impregnated gelatin microbeads into the wound bed. After the implantation of the artificial dermis, the extent of epidermal tissue regeneration over the artificial dermis was evaluated and compared with that of an artificial dermis containing MIF-free hydrogel microbeads. Seven days after implantation, the mice were sacrificed and the artificial dermis and the surrounding tissue harvested. After removal, tissues were immediately embedded and frozen in Tissue-Tek OCT compound (Miles Scientific), and 4-μm-thick sections cut. Microvessel staining for CD31 was then performed. Briefly, the tissue sections were incubated with rat anti-mouse CD31 antibody diluted 1:500 overnight at 4°C. Specific binding was detected through avidin-biotin-peroxidase complex formation using a biotin-conjugated goat anti-rat IgG (Vectastain ABC kit; Vector Laboratories, Burlingame, CA) and diaminobenzidine as a chromogen substrate. Counterstaining using hematoxylin to detect nuclei was performed. Seven days after implantation of the artificial dermis, CD31-positive cells were assessed by light microscopy in areas of the implanted, artificial dermis, and the number of these positive cells was determined in six fields at ×200 magnification (n = 10 in each group). Similarly, the microvessel density evaluation in the tissue samples was also performed by measuring the number of capillaries in six fields at ×200 magnification (n = 10 in each group). For mRNA analysis, artificial dermis at 7 days was harvested, snap-frozen, and stored at −80°C. All experiments were repeated three times.

Western Blot Analysis

Skin at the wounded edge (5 mm around the wound) was disrupted and homogenized with a Polytron homogenizer (Kinematica, Lausanne, Switzerland). The protein concentrations of the cell homogenates were quantified using a Micro BCA protein assay reagent kit. Equal amounts of homogenates were dissolved in 20 μl of Tris-HCl, 50 mmol/L (pH 6.8), containing 2-mercaptoethanol (1%), sodium dodecyl sulfate (SDS) (2%), glycerol (20%), and bromophenol blue (0.04%), and the samples were heated to 100°C for 5 minutes. The samples were then subjected to SDS-polyacrylamide gel electrophoresis (PAGE) and electrophoretically transferred onto a nitrocellulose membrane. The membranes were blocked with 1% nonfat dry milk powder in phosphate-buffered saline (PBS), probed with anti-MIF antibodies and subsequently reacted with secondary goat anti-rabbit IgG antibodies coupled with horseradish peroxidase. The resultant complexes were processed for the detection system according to the manufacturer's protocol (Cell Signaling Technology, Beverly, MA).

ELISA

The ELISA was performed as previously described.[15] Briefly, the anti-rat MIF antibody was added to each well of a 96-well microtiter plate and left for 1 hour at room temperature. Before the addition of the antibody, all wells had been filled with PBS containing bovine serum albumin (1%) for blocking and left for 1 hour at room temperature. Samples were then added in duplicate to individual wells and incubated for 1 hour at room temperature. After the plate was washed three times with PBS containing 0.05% Tween 20 (washing buffer), samples were again added in duplicate to individual wells and incubated for 1 hour at room temperature. After the plate was washed three times, 50 μl of biotin-conjugated anti-MIF antibody (IgG fraction) was added to each well. After incubation for1 hour at room temperature, the plate was again washed three times with washing buffer. Then, avidin-conjugated horseradish peroxidase was added to each well, followed by addition of IgG antibody and incubation for 1 hour at room temperature. Fifty μl of substrate containing *o*-phenylenediamine and hydrogen peroxide in citrate-phosphate buffer (pH 5.0) were added to each well. After incubation for 20 minutes at room temperature, the reaction was stopped with sulfuric acid, and the absorbance at 492 nm was measured using an ELISA plate reader (model 3550; Bio-Rad, Hercules, CA).

Reverse Transcriptase-Polymerase Chain Reaction (RT-PCR) Analysis

The fibroblasts from WT mice were incubated with or without LPA (0 to 10 μmol/L). Total RNA was extracted with an Isogen RNA extraction kit (Nippon Gene) according to the protocol provided by the manufacturer, and MIF mRNA expression was analyzed. The reverse transcription of the RNA was performed with M-MLV reverse transcriptase using a random hexamer primer and subsequent amplification using *Taq*DNA polymerase. PCR was performed for 35 cycles with denaturation at 94°C for 1 minute, annealing from 55 to 65°C for 1 minute, and extension at 72°C for 1 minute using a thermal cycler (Gene Amp PCR system 9700; PE Applied Biosystems). MIF primers used were 5′-GTTTCTGTCGGAGCTCAC-3′ (55 to 72) (forward) and 5′-AGCGAAGGTGGAACCGTTCCA-3′ (215 to 236) (reverse). Glyceraldehyde-3-phosphate dehydrogenase (GAPDH) was used as a positive control. Primers used were 5′-GAAGGTCGGTGTGAACGGATTTG-3′ (6 to 28) (forward) and 5′-GTCCACCACCCTGTTGCTGTAGC-3′ (949 to 971) (reverse). After PCR, the amplified products were analyzed by 2% agarose gel electrophoresis.

Northern Blot Analysis

Total cellular RNA was isolated from MIF-impregnated artificial dermis or control artificial dermis using an Isogen extraction kit according to the manufacturer's protocols. RNA (10 μg) was resuspended in TE (10 mmol/L Tris-HCl, 1 mmol/L ethylenediamine tetraacetic acid, pH 7.4), and denatured and electrophoresed on 1% agarose formaldehyde gel. The RNA was then transferred to nylon membranes and cross-linked by UV irradiation. Prehybridization was performed in 0.75 mol/L NaCl, 0.02 mol/L Tris-HCl (pH7.5), 2.5 mmol/L ethylenediamine tetraacetic acid, 0.5× Denhardt's solution, 1% SDS, and 50% formamide at 42°C for 4 hours. Then hybridization was performed in the same buffer containing 10% dextran sulfate, salmon sperm DNA (250 μg/ml), and a radiolabeled probe at 42°C for 20 hours. The radiolabeled probe was prepared using human procollagen α1 or vascular endothelial growth factor (VEGF) cDNA as a template and labeled with a random primer labeling kit using [α-^{32}P]dCTP. Procollagen α_1 primers used were 5′AAAGGCTGGAGAGCGA-3′, and the reverse primer was 5′ AGCAGGACCTGGGGGA-3′.[29] VEGF (826 bp) primers used were 5′-GGA CCC TGG CTT TAC TGC-3′ (forward) and 5′-CGG GCT TGG CGA TTT AG-3′ (reverse).[30] The membrane was washed twice with 2× standard saline citrate (16.7 mmol/L NaCl, 16.7 mmol/L sodium citrate) at 22°C for 5 minutes, twice with 0.2× standard saline citrate containing 0.1% SDS at 65°C for 15 minutes, and twice with 2× standard saline citrate at 22°C for 20 minutes before autoradiography. Quantitative densitometric analysis was performed using an MCID image analyzer (Fuji Film, Tokyo, Japan). The density of VEGF and procollagen α_1 bands was normalized by the intensities of GAPDH.

Statistical Analysis

Differences between the various treatments were statistically tested using the Student's *t*-test and the Mann-Whitney *U*-test. For comparisons of multiple groups, one-way analysis of variance was applied to the data. *P* values of <0.05 were considered statistically significant. Data in the figures are shown as the mean ± SEM of several experiments.

Results

Wound Healing and Skin Chemokine Expression in MIF-Deficient Mice

We first examined whether MIF is important in the cutaneous wound-healing process *in vivo* using MIF KO mice. The number of mice showing complete healing of four skin lesions was plotted at different time points after penetrating (full thickness) wounds through both epidermis and dermis. Fifteen MIF KO and WT mice were examined in each group. After the excision of a 5-mm-diameter round wound from dorsal skin of MIF KO mice and WT mice, healing was significantly delayed in MIF KO mice compared to WT mice (Figure 1a) ($P < 0.0001$). Healing was apparently delayed in MIF KO mice compared with that of WT mouse skin (Figure 1b). Wounded MIF KO mice appeared to induce significantly less granulation tissue formation compared to WT mice.

Fibroblast Proliferation, Apoptosis, and Collagen-Gel Contraction in MIF KO Mice

An important step in wound repair is the infiltration of fibroblasts into the wound site, where fibroblasts synthesize extracellular matrix components and remodel the damaged tissue. Fibroblast proliferation is an essential event during wound repair. LPS treatment at a concentration more than 0.05 μg/ml in the culture medium significantly increased [^{3}H]thymidine uptake in WT mice, when compared to the effects in MIF KO mice fibroblasts after incubation throughout 3 days (Figure 2a). The possibility remains that reduced fibroblast proliferation may reflect cell apoptosis in MIF KO mice. We therefore measured the induction of apoptosis after LPS stimulation using the TUNEL assay. Stimulation with LPS had little effect on fibroblast apoptosis on both MIF KO and WT mice (Figure 2b). These results confirmed previous reports that LPS does not directly induce fibroblast apoptosis.[31] Another important event during wound healing is contraction of the newly formed granulation tissue wound bed by fibroblasts to bring together the edges of the wound. Type I collagen diameter was measured at various time points after incorporation of fibroblasts in the collagen gel, and WT mouse fibroblasts showed a significantly greater contractile property compared with MIF KO fibroblasts ($P < 0.01$) (Figure 2c).

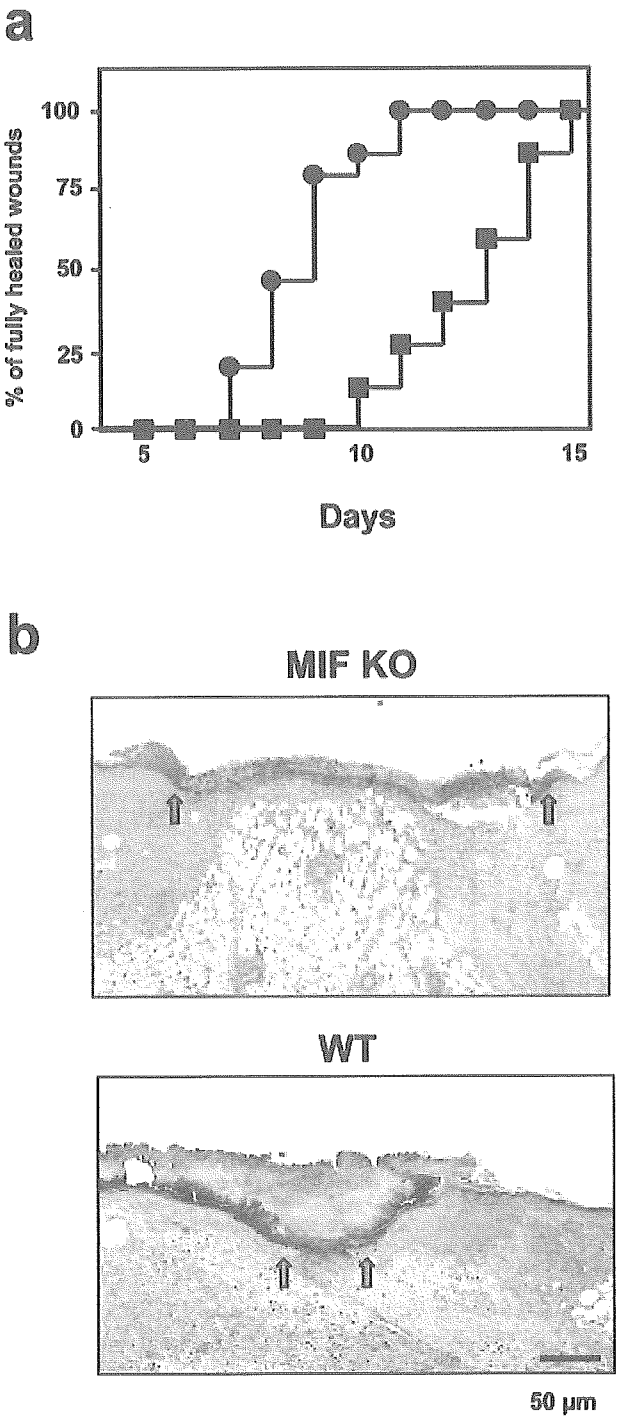

Figure 1. Wound healing in the skin of MIF KO mice. **a:** The percentage frequency of completely healed skin lesion was plotted at different time points after skin wounding. Fifteen MIF KO (■) and WT mice (●) were examined in each group after the excision of a 5-mm biopsy wound from dorsal skin. MIF KO versus WT mice; $P < 0.0001$. **b:** Microphotograph taken at 5 days after wounding in MIF KO and WT mouse. Healing was apparently delayed in MIF KO mouse compared with that of WT mouse skin. Wound margins indicated by **arrows**. Scale bar, 50 μm.

MIF KO Mouse Fibroblast and Keratinocyte Migration

We next examined whether MIF had the potential to affect fibroblast and keratinocyte migration. Skin fibroblasts and keratinocytes were obtained from MIF KO and WT mice. After the initial plating of the fibroblasts, cells were scraped off using a yellow pipette tip (*in vitro* wound). Subsequently at 6 and 12 hours, the numbers of migrating cells from the baseline were measured after 10-μmol/L LPA stimulation. The result showed that an increase in fibroblast migration was observed in WT mice fibroblasts compared to MIF KO mice cells at both 6 and 12 hours after LPA stimulation ($^*P < 0.005$) (Figure 3, a and b). The decreased cell motility in MIF KO fibroblasts was further confirmed by a Boyden chamber assay. Indeed, MIF KO mouse fibroblasts showed a reduced ability to migrate through 8-μm pore-sized membranes ($P < 0.001$) (Figure 3c). Keratinocyte migration was also ana-

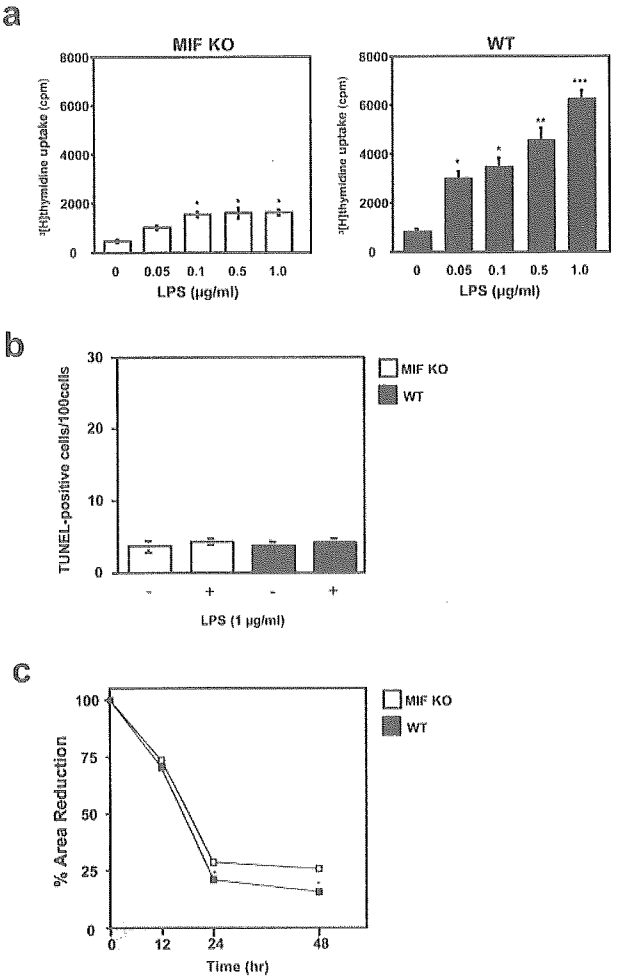

Figure 2. Proliferation and apoptosis in MIF KO mouse cultured fibroblasts after LPS treatment. **a:** Fibroblasts were incubated with the indicated concentrations of LPS for 3 days and pulsed with [^{3}H]thymidine. [^{3}H]thymidine incorporation into DNA was determined. LPS treatment significantly stimulated cultured fibroblast proliferation in WT mice compared to MIF KO mice fibroblasts. Results are expressed as mean ± SEM of three experiments performed in duplicate. $^*P < 0.05$, $^{**}P < 0.001$, $^{***}P < 0.0005$. **b:** Quantitative analysis of fibroblast apoptosis after LPS stimulation. The number of TUNEL-positive cells was counted in WT mice, and compared with MIF KO mouse fibroblasts. Both MIF KO and WT mouse fibroblasts showed few apoptotic cells after LPS treatments. Each value represents the mean ± SEM of six specimens. **c:** Contraction of collagen gels by WT and MIF KO fibroblasts. Cells were incorporated in collagen gels and incubated in DMEM plus 2% fetal bovine serum and contraction was monitored for 48 hours. The area of gels was calculated from the average diameter of the experiments and expressed as a percentage of the initial area. Results are expressed as mean ± SEM of six experiments. $^*P < 0.01$.

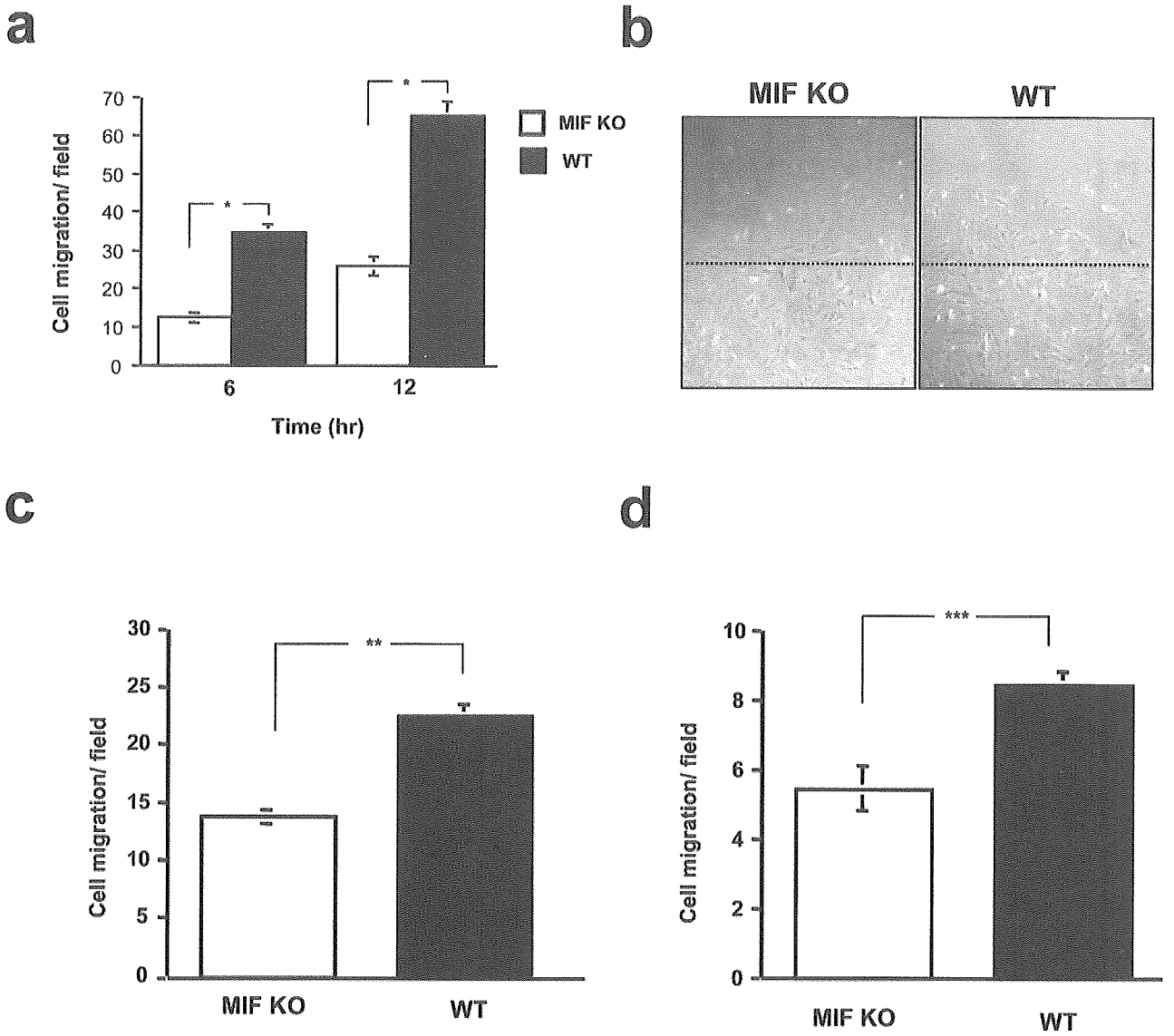

Figure 3. Migration of MIF KO mouse cultured fibroblasts or keratinocytes after LPA stimulation. **a:** After the initial plating of fibroblasts obtained from both MIF KO and WT mice, the cells were scraped off. Subsequently at 6 and 12 hours, the numbers of cells migrating into the cleared area from the baseline were measured after addition of LPA (10 μmol/L) to the medium. Results are expressed as mean ± SEM of five different experiments. $^{*}P < 0.005$. **b:** Representative migration rates for cultured fibroblasts are depicted after 6 hours of fibroblast migration. Migration of MIF KO fibroblasts was reduced in comparison to WT mice. **Dashed line** indicates the edge of the wound created at 0 hours. **c:** The Boyden chamber assay was performed using 8-μm pore-sized membranes. Migration activity was quantified by blind counting of the migrating cells on the lower surface of the membrane in 10 high-power microscope fields per chamber using a ×100 objective. The difference in fibroblast migration levels between MIF KO and WT mice was statistically significant ($^{**}P < 0.001$). (This experiment was repeated a third time with similar results.) **d:** Chemotaxis of keratinocytes in response to LPA (10 μmol/L) was performed using a Boyden chamber assay as described above. The difference in keratinocyte migration levels between MIF KO and WT mice was statistically significant ($^{***}P < 0.001$). (This experiment was repeated a third time with similar results.)

lyzed by Boyden chamber assay. A significantly lower keratinocyte migration was observed in MIF KO mice, compared to that of WT mice ($P < 0.001$) (Figure 3d).

LPA-Induced Rho GTPase Activation

We then examined whether LPA could induce MIF mRNA expression in normal C57BL/6 mouse fibroblasts. The result showed that LPA-induced MIF mRNA expression in mouse fibroblasts was dose-dependent (Figure 4a). Next, we measured the intracellular levels of the GTP-bound active forms of Rho family using the pull-down assay system. In WT mouse fibroblasts, the level of GTP-bound RhoA, Rac1, and Cdc42 was elevated after the addition of LPA and reached a peak 15 minutes after LPA addition, whereas activated GTP-Rho family proteins (RhoA, Rac1, and Cdc42) were significantly reduced in MIF KO mouse fibroblasts after LPA treatment (Figure 4b).

Recovery of Normal Wound-Healing Rate after Treatment with MIF-Impregnated Gelatin Microbeads

To examine whether exogenous MIF could accelerate wound healing, we used MIF-impregnated gelatin mi-

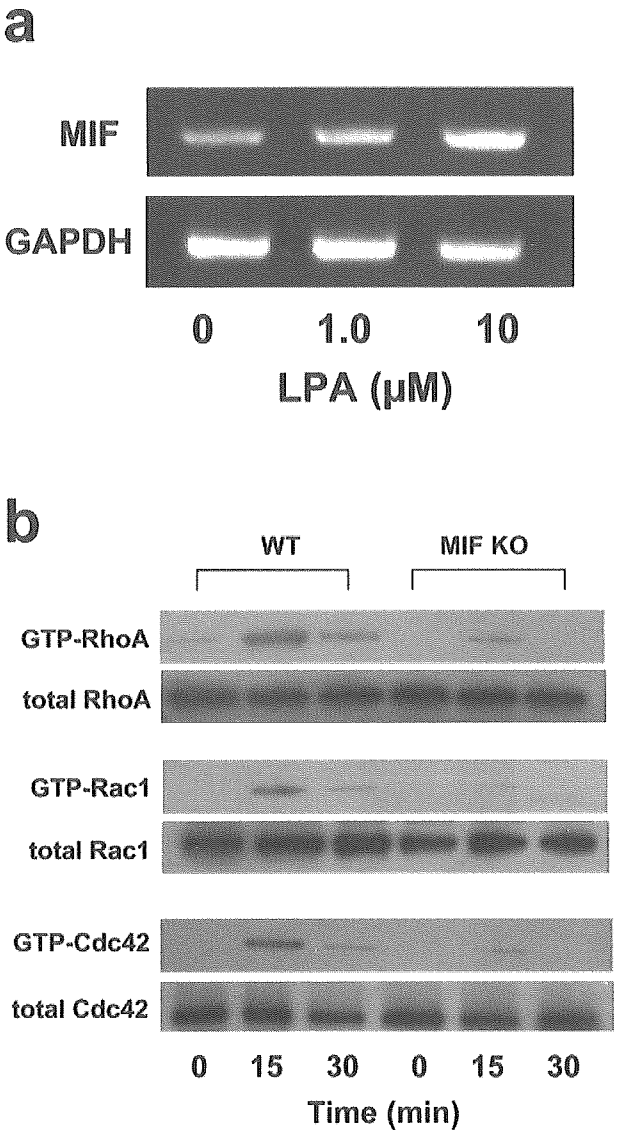

Figure 4. MIF mRNA expression and RhoA activation induced by LPA in MIF KO mouse skin fibroblasts. **a:** RT-PCR analysis of the expression of MIF mRNA in response to LPA. LPA (0, 1.0, and 10 μmol/L) was added to the medium of normal C57BL/6 fibroblasts. After 24 hours, the total RNA was extracted and subjected to RT-PCR analysis. **b:** Activated GTP-RhoA, GTP-Cdc42, and GTP-Rac1 in C57BL/6 fibroblasts were assayed by Western blotting. Cells were stimulated with LPA (10 μmol/L) for 0 to 30 minutes. Aliquots of respective lysates served as controls for analyzing the total amount of RhoA, Rac1, and Cdc42 protein. The data shown are representative of two independent experiments.

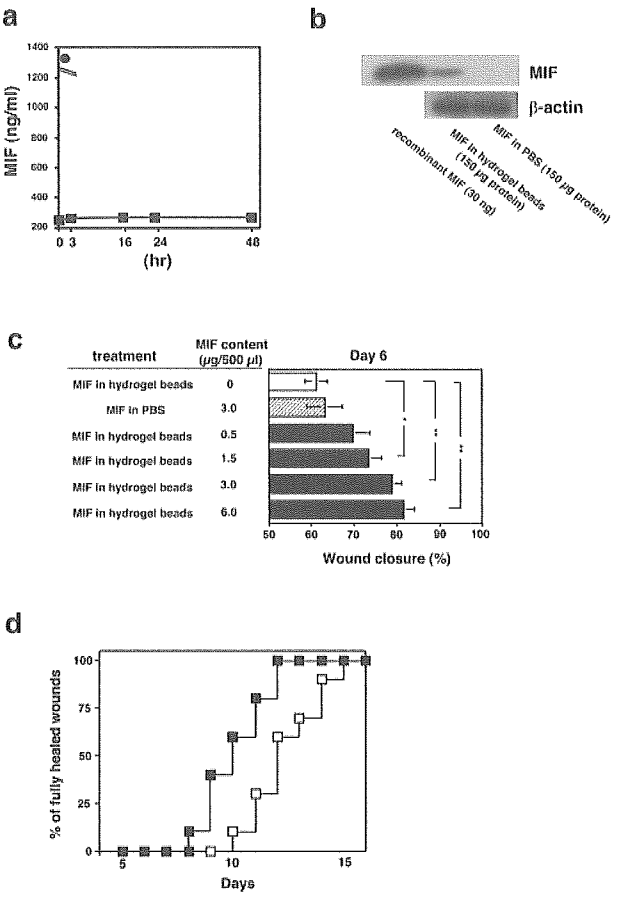

Figure 5. Recovery of normal rates of wound healing after treatment with MIF-impregnated gelatin hydrogel microbeads in MIF KO mice. **a:** MIF-impregnated gelatin microbeads (30 μg MIF in 2 mg of gelatin beads) dissolved in 6 ml of PBS were stored for 48 hours. Then, the MIF content of the solution/medium was determined by MIF ELISA. MIF-impregnated gelatin microbeads (■) and free MIF (30 μg/20 μl) were dissolved in 6 ml of PBS (●). **b:** MIF (3 μg/500 μl) in hydrogel microbeads or 3 μg/500 μl of MIF in PBS without hydrogel microbeads were injected to a dermal area of the back of MIF KO mice on day 0. On day 10, a central area of skin (5 × 5 mm in diameter) was obtained and subjected to Western blot analysis (150 μg protein in each group). The data shown are representative of three independent experiments. **c:** MIF (0 to 6 μg/500 μl) in hydrogel beads were injected around the wound edge of MIF KO mice (n = 10 in each group). For controls, a solution containing 3 μg/500 μl of MIF in PBS without hydrogel beads were injected around the wound edges (n = 10). On day 6, the percentage of wound closure was examined (n = 10 × 4 in each group). $^{*}P < 0.05$, $^{**}P < 0.005$. **d:** Frequency of completely healed skin lesions was plotted at different time points after skin wound (n = 10 in each group); (■), 3 μg/500 μl of MIF-impregnated gelatin microbeads injection group and (□), 3 μg/500 μl of MIF in PBS injection without gelatin microbeads group. $P <$ 0.005 for MIF-impregnated gelatin microbeads versus MIF in PBS.

crobeads in the next series of experiments. We first examined the *in vitro* release of recombinant MIF from within the acidic gelatin hydrogel microbeads. Approximately, 5% of the MIF was released into the PBS buffer solution within the initial 1 hour after the start of the test, but thereafter, no substantial release was observed until 48 hours (Figure 5a). To confirm whether MIF was released from the hydrogel microbeads *in vivo*, 3 μg/500 μl of the MIF-containing hydrogel microbeads or 3 μg/500 μl of MIF in PBS without hydrogel microbeads were injected into the back skin (10 mm in diameter) of the MIF KO mice on day 0. On day 10, the central area of skin was removed and subjected to Western blot analysis. The data demonstrated that MIF was detected in the skin in the MIF hydrogel microbead-treated group by Western blot analysis (Figure 5b). Conversely, MIF levels in the PBS-treated group showed no detectable background levels of MIF.

We next examined the effect of MIF-impregnated gelatin microbeads around the skin wounds. Concentrations of MIF (0 to 6.0 μg/500 μl) incorporated into hydrogel microbeads were injected around the edge of wounds on the back of MIF KO mice at day 1. As a control, 3 μg/500 μl of MIF in PBS not associated with hydrogel microbeads was injected directly into or around the wound edges. On day 6, extent of epidermal wound closure was

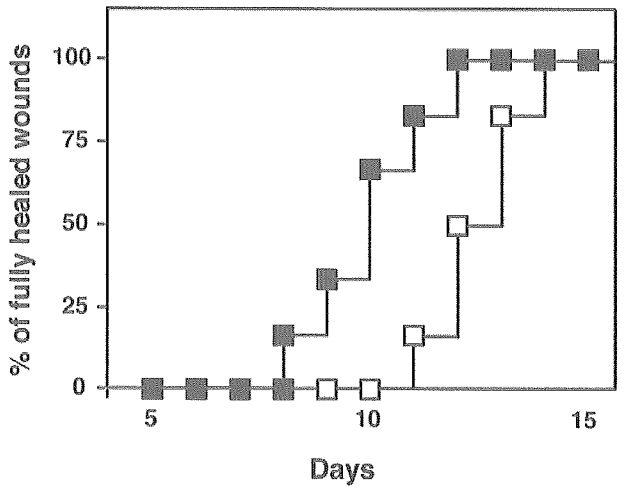

Figure 6. Recovery of wound healing after treatment with MIF-impregnated gelatin hydrogel microbeads in *db/db* mice. Frequency of completely healed skin lesions was plotted at different time points after skin wounding ($n = 6$ in each group); (■), 3 μg/500 μl of MIF-impregnated gelatin microbeads application treatment group and (□), 3 μg/500 μl of MIF in PBS direct injection group (without using gelatin microbeads). $P < 0.05$ for MIF-impregnated gelatin microbeads versus MIF in PBS treatments.

measured (as a percentage of the initial wound area). Significantly faster wound closure was observed after treatment in groups treated with more than 1.5 μg/500 μl of MIF hydrogel microbeads compared with the untreated group and the group that was directly injected with MIF (3 μg/500 μl) in PBS (*$P < 0.05$ and **$P < 0.005$, respectively) (Figure 5c). Complete healing was seen between 8 and 12 days in the 3.0 μg/500 μl of MIF hydrogel microbead-treated group, whereas it was observed between 10 and 15 days for mice directly injected with 3 μg/500 μl of MIF/PBS ($P < 0.005$) (Figure 5d).

To test whether MIF-impregnated gelatin microbeads are useful for optimizing wound healing in C57BL/6 and diabetic model (*db/db*) mice, we analyzed the effect of MIF-impregnated gelatin microbeads around wounded skin in control/WT C57BL/6 mice and *db/db* mice, a rodent model of type 2 diabetes. Complete wound closure was observed after 6.6 ± 0.3 days in the MIF (3 μg/500 μl)-impregnated gelatin microbead-treated group, whereas it was seen on day 8.3 ± 0.3 in control group (3 μg/500 μl of MIF in PBS) ($n = 6$ in each group, $P < 0.01$). Similar results were also observed when we used *db/db* mice. Complete wound closure was seen between 8 and 12 days in the 3.0 μg/500 μl of MIF hydrogel microbead-treated group, whereas it was observed between 11 and 14 days for mice directly injected with 3 μg/500 μl of MIF/PBS ($P < 0.05$) (Figure 6). These facts indicate that MIF-containing hydrogel microbeads are better at stimulating wound healing more than direct MIF injection.

Accelerated Tissue Regeneration after Incorporation of MIF-Impregnated Gelatin Microbeads into an Artificial Dermis in MIF KO Wounded Mice

Angiogenesis and collagen synthesis are important in wound repair. Seven days after the implantation of an artificial dermis into MIF KO mice, the implanted artificial dermis and the surrounding tissue were harvested. Then, the implanted artificial tissue samples from each experimental group then underwent CD31-positive cell counts and microvessel density evaluation. All endothelial cells were stained with anti-rat CD31 antibody. After MIF-impregnated gelatin microbead treatment, the artificial dermis showed a statistically significantly higher CD31-positive cell count and microvessel density when compared with control artificial dermis treated with gelatin microbeads without MIF ($P < 0.0001$) (Figure 7, a and b). Northern blot analysis of the mRNA levels in MIF-impregnated artificial dermis showed enhanced procollagen α1

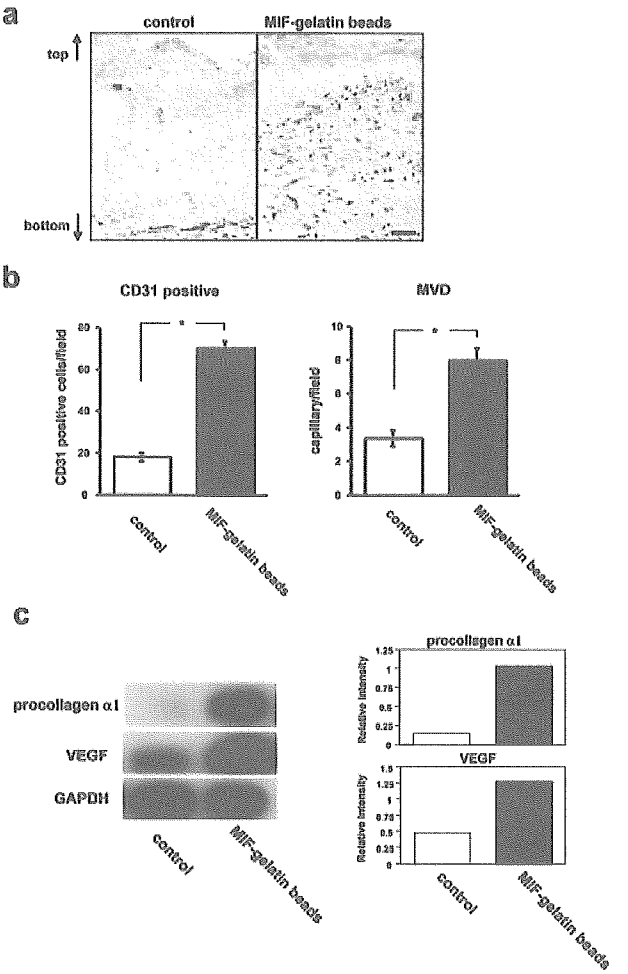

Figure 7. Counting of CD31-positive cells and RT-PCR analysis of procollagen α1 and VEGF in artificial dermis of the MIF-impregnated gelatin microbead-treated group in MIF KO mice. **a:** Cryostat sections of artificial dermis 7 days after implantation were stained with anti-CD31 antibody and representative sections were shown of MIF-free gelatin microbeads-only treated group implanted into an artificial dermis (control) and MIF-impregnated gelatin microbead-treated group placed into an artificial dermis. **Arrows** show the vertical orientation of the artificial dermis. **b:** The frequency of CD31-positive cells and microvessel density evaluation were performed in the artificial dermis using views from six fields at ×200 ($n = 10$ in each group). *$P < 0.0001$. (This experiment was repeated a third time with similar results.) **c:** The increase in procollagen α1 and VEGF mRNA levels in the artificial dermis of the MIF-impregnated gelatin microbead-treated group were compared with the control group (artificial dermis without MIF) by Northern blot analysis on day 7. The density of procollagen α1 and VEGF was normalized to the GAPDH signal. Scale bar, 50 μm (**a**).

and VEGF expression when compared with control artificial dermis (Figure 7c).

Discussion

The wound repair process is a highly ordered series of events that encompasses hemostasis, inflammatory cell infiltration, tissue regrowth, and remodeling. An important process in normal wound healing is the generation of an inflammatory reaction, which is characterized by the deposition of platelets and the sequential infiltration of neutrophils, macrophages, and lymphocytes.[32] It is known that various growth factors, cytokines, and chemokines function in the wound-healing process.[1,33] Genetically modified mouse studies have helped to elucidate the roles that many cytokines and chemokines play during wound repair.[34] Excisional wounds in IL-6 KO mice took up to three times longer to heal than those of WT mice, and were characterized by a dramatic delay in re-epithelization and granulation tissue formation.[35] IL-6 is a pleiotropic cytokine that is involved in the growth and differentiation of numerous cell types, and is mitogenic for keratinocytes. Recently, one of the chemokine KO models (MCP-$1^{-/-}$) also showed significantly delayed wound re-epithelization, angiogenesis, and collagen synthesis.[36]

MIF was originally identified as a proinflammatory cytokine. Now, MIF is known to be involved in a variety of biological processes, including cell proliferation, angiogenesis, and chemotactic effects in cells.[9,10] In the present study, we have shown that wound healing was significantly delayed in MIF KO mice compared to WT mice. Wounds in MIF KO mice seemed to induce significantly less granulation tissue formation compared to WT mice. LPS treatment significantly increased cultured fibroblast proliferation in WT mice compared to MIF KO mouse fibroblasts. Moreover, we have demonstrated that MIF KO skin fibroblasts contracted collagen lattices more slowly than WT mice fibroblasts. Because fibroblasts synthesize the matrix components that comprise granulation tissue, we regard a deficiency in fibroblast matrix synthesis as one possible cause of wound repair delay. Additionally, a significant increase in fibroblast and keratinocytes migration was observed in WT mice compared to MIF KO mice. Excessive expression of MIF may directly or indirectly stimulate cell proliferation, contracted collagen lattices, and migration, which profoundly modulate the wound-healing process. LPA is a product of activated platelets and white cells and has diverse actions on target cells. LPA is a mitogen for a number of cell types, including fibroblasts.[37] In general, cell migration is driven by signaling pathways controlled by the Rho family GTPases, RhoA, Rac1, and Cdc42, acting in a coordinated manner.[38] We found that LPA-induced MIF mRNA expression was up-regulated in fibroblasts because LPA activates Rho family GTPases in WT mice fibroblasts but not in MIF KO fibroblasts. These results indicate that MIF is important in fibroblast migration in a Rho GTPase-dependent manner.

We previously found that neutralizing anti-MIF antibody significantly delayed skin wound healing, suggesting the involvement of MIF in skin regeneration after wounding.[15] In this report, we further confirmed the participation of MIF in the skin wounds using MIF KO mice that showed delayed wound healing compared with WT mice. In contrast, Ashcroft and colleagues[19] reported that no difference in the rate of healing was observed between MIF KO and WT mice. The reason why this contrary result was obtained is currently unclear, although, it might be assumed that some differences in experimental procedure may lead to this result. For example, the wound-healing protocols were different, as we examined full wound closure (four full-thickness 5-mm-diameter round wounds) extensively during which process of skin regeneration is completed, whereas they judged wound healing on day 3, 7, and 14 after wounding (two equidistant 1-cm full-thickness incision wounds).[19]

We have also demonstrated the sustained release of MIF using slow-release gelatin microbeads accelerates the process of wound healing. These MIF-impregnated gelatin microbeads might not only be useful for correcting MIF KO mice but also enhance normal C57BL/6 mice and diabetic model mice (*db/db* mice) rates of wound healing. The time course during which the protein is released correlates with the rate of hydrogel degradation.[39] It is very likely that the protein-drug complex associated with the gelatin hydrogel, is released as a result of its biodegradation. Thus the gelatin hydrogel system releases the protein drug only under conditions in which there is maintenance of biological activity. Therefore, sustained release of the growth factor from the gelatin hydrogel is made more effective in exerting its biological functions under our test conditions.[39] Our studies further demonstrated that the use of MIF-impregnated gelatin microbeads in mouse skin with defective MIF increased both the levels of angiogenesis and of collagen mRNA expression, compared with control artificial dermis undergoing comparable control saline treatment. This artificial dermis has previously been used for the treatment of full-thickness skin defects resulting from injures and burns. It is well known that VEGF especially has many biological activities that stimulate capillary endothelial cells and promote angiogenesis.[40] Previously Chesney and colleagues[41] and we[42] demonstrated that MIF induced angiogenesis and that MIF also up-regulated VEGF expression. Taken together, these results suggest that wound-associated MIF production plays an important, functional role in neovascularization and in the development of granulation tissue, both of which are key events in wound repair. In addition to these findings, gelatin microbeads containing MIF continue to show considerable promise in treatment to accelerate the rate of skin wound healing.

Acknowledgment

We thank Dr. James R. McMillan for proofreading the manuscript.

References

1. Werner S, Grose R: Regulation of wound healing by growth factors and cytokines. Physiol Rev 2003, 83:835–870
2. Feiken E, Romer J, Eriksen J, Lund LR: Neutrophils express tumor necrosis factor-alpha during mouse skin wound healing. J Invest Dermatol 1995, 105:120–123
3. Hubner G, Brauchle M, Smola H, Madlener M, Fassler R, Werner S: Differential regulation of pro-inflammatory cytokines during wound healing in normal and glucocorticoid-treated mice. Cytokine 1996, 8:548–556
4. Wetzler C, Kampfer H, Stallmeyer B, Pfeilschifter J, Frank S: Large and sustained induction of chemokines during impaired wound healing in the genetically diabetic mouse: prolonged persistence of neutrophils and macrophages during the late phase of repair. J Invest Dermatol 2000, 115:245–253
5. Bloom BR, Bennett B: Mechanism of a reaction in vitro associated with delayed-type hypersensitivity. Science 1966, 153:80–82
6. David JR: Delayed hypersensitivity in vitro: its mediation by cell-free substances formed by lymphoid cell-antigen interaction. Proc Natl Acad Sci USA 1996, 56:72–77
7. Bernhagen J, Calandra T, Mitchell RA, Martin SB, Tracey KJ, Voelter W, Manogue KR, Cerami A, Bucala R: MIF is a pituitary-derived cytokine that potentiates lethal endotoxemia. Nature 1993, 365:756–759
8. Calandra T, Bernhagen J, Mitchell RA, Bucala R: The macrophage is an important and previously unrecognized source of macrophage migration inhibitory factor. J Exp Med 1994, 179:1895–1902
9. Bucala R: MIF re-discovered: pituitary hormone and glucocorticoid-induced regulator of cytokine production. FASEB J 1996, 7:19–24
10. Nishihira J: Macrophage migration inhibitory factor (MIF): its essential role in the immune system and cell growth. J Interferon Cytokine Res 2000, 20:751–762
11. Nishio Y, Minami A, Kato H, Kaneda K, Nishihira J: Identification of macrophage migration inhibitory factor (MIF) in rat peripheral nerves: its possible involvement in nerve regeneration. Biochim Biophys Acta 1999, 1453:74–82
12. Shimizu T, Abe R, Ohkawara A, Nishihira J: Increased production of macrophage migration inhibitory factor by PBMCs of atopic dermatitis. J Allergy Clin Immunol 1999, 104:659–664
13. Shimizu T: Role of macrophage migration inhibitory factor (MIF) in the skin. J Dermatol Sci 2005, 37:65–73
14. Shimizu T, Abe R, Ohkawara A, Nishihira J: Ultraviolet B radiation upregulates the production of macrophage migration inhibitory factor (MIF) in human epidermal keratinocytes. J Invest Dermatol 1999, 112:210–215
15. Abe R, Shimizu T, Ohkawara A, Nishihira J: Enhancement of macrophage migration inhibitory factor (MIF) expression in injured epidermis and cultured fibroblasts. Biochim Biophys Acta 2000, 1500:1–9
16. Roger T, Glauser MP, Calandra T: Macrophage migration inhibitory factor (MIF) modulates innate immune responses induced by endotoxin and Gram-negative bacteria. J Endotoxin Res 2001, 7:456–460
17. Shimizu T, Ohkawara A, Nishihira J, Sakamoto W: Identification of macrophage migration inhibitory factor (MIF) in human skin and its immunohistochemical localization. FEBS Lett 1996, 381:199–202
18. Shimizu T, Nishihira J, Watanabe H, Abe R, Honda A, Ishibashi T, Shimizu H: Macrophage migration inhibitory factor (MIF) is induced by thrombin and factor Xa in endothelial cells. J Biol Chem 2004, 279:13729–13737
19. Ashcroft GS, Mills SJ, Lei K, Gibbons L, Jeong MJ, Taniguchi M, Burow M, Horan MA, Wahl SM, Nakayama T: Estrogen modulates cutaneous wound healing by downregulating macrophage migration inhibitory factor. J Clin Invest 2003, 111:1309–1318
20. Honma N, Koseki H, Akasaka T, Nakayama T, Taniguchi M, Serizawa I, Akahori H, Osawa M, Mikayama T: Deficiency of the macrophage migration inhibitory factor gene has no significant effect on endotoxaemia. Immunology 2000, 100:84–90
21. Ortega S, Ittmann M, Tsang SH, Ehrlich M, Basilico C: Neuronal defects and delayed wound healing in mice lacking fibroblast growth factor 2. Proc Natl Acad Sci USA 1998, 95:5672–5677
22. Denon D, Kowatch MA, Roth GS: Production of wound repair in old mice by local injection of macrophages. Proc Natl Acad Sci USA 1989, 86:2018–2020
23. Basu A, Kligman LH, Samulewicz SJ, Howe CC: Impaired wound healing in mice deficient in a matricellular protein SPARC (osteonectin, BM-40). BMC Cell Biol 2001, 2:15
24. Mannino RJ, Ballmer K, Zeltner D, Burger MM: An inhibitor of animal cell growth increases cell-to-cell adhesion. J Cell Biol 1981, 91:855–859
25. Benard V, Bohl BP, Bokoch GM: Characterization of rac and cdc42 activation in chemoattractant-stimulated human neutrophils using a novel assay for active GTPases. J Biol Chem 1999, 274:13198–13204
26. Ikada Y, Tabata Y: Protein release from gelatin matrices. Adv Drug Deliv Rev 1998, 31:287–301
27. Kawai K, Suzuki S, Tabata Y, Ikada Y, Nishimura Y: Accelerated tissue regeneration through incorporation of basic fibroblast growth factor-impregnated gelatin microspheres into artificial dermis. Biomaterials 2000, 21:489–499
28. Yamamoto M, Ikada Y, Tabata Y: Controlled release of growth factors based on biodegradation of gelatin hydrogel. J Biomater Sci Polym Ed 2001, 12:77–88
29. McGaha TL, Le M, Kodera T, Stoica C, Zhu J, Paul WE, Bona CA: Molecular mechanisms of interleukin-4-induced up-regulation of type I collagen gene expression in murine fibroblasts. Arthritis Rheum 2003, 48:2275–2284
30. Nalbandian A, Dettin L, Dym M, Ravindranath N: Expression of vascular endothelial growth factor receptors during male germ cell differentiation in the mouse. Biol Reprod 2003, 69:985–994
31. Alikhani M, Alikhani Z, He H, Liu R, Popek BI, Graves DT: Lipopolysaccharides indirectly stimulate apoptosis and global induction of apoptotic genes in fibroblasts. J Biol Chem 2003, 278:52901–52908
32. Martin P: Wound healing—aiming for perfect skin regeneration. Science 1997, 276:75–81
33. Shah M, Foreman DM, Ferguson MW: Neutralisation of TGF-beta 1 and TGF-beta 2 or exogenous addition of TGF-beta 3 to cutaneous rat wounds reduces scarring. J Cell Sci 1995, 108:985–1002
34. Grose R, Werner S: Wound-healing studies in transgenic and knockout mice. Mol Biotechnol 2004, 28:147–166
35. Gallucci RM, Simeonova PP, Matheson JM, Kommineni C, Guriel JL, Sugawara T, Luster MI: Impaired cutaneous wound healing in interleukin-6-deficient and immunosuppressed mice. FASEB J 2000, 14:2525–2531
36. Low QE, Drugea IA, Duffner LA, Quinn DG, Cook DN, Rollins BJ, Kovacs EJ, DiPietro L: Wound healing in MIP-1alpha(−/−) and MCP-1(−/−) mice. Am J Pathol 2001, 159:457–463
37. O'Connor KL, Shaw LM, Mercurio AM: Release of cAMP gating by the alpha6beta4 integrin stimulates lamellae formation and the chemotactic migration of invasive carcinoma cells. J Cell Biol 1998, 143:1749–1760
38. Nobes CD, Hall A: Rho GTPases control polarity, protrusion, and adhesion during cell movement. J Cell Biol 1999, 144:1235–1244
39. Tabata Y: Tissue regeneration based on growth factor release. Tissue Eng 2003, 9(Suppl 1):S5–S15
40. Pierce GF, Tarpley JE, Yanagihara D, Mustoe TA, Fox GM, Thomason A: Platelet-derived growth factor (BB homodimer), transforming growth factor-beta 1, and basic fibroblast growth factor in dermal wound healing. Neovessel and matrix formation and cessation of repair. Am J Pathol 1992, 140:1375–1388
41. Chesney J, Metz C, Bacher M, Peng T, Meinhardt A, Bucala R: An essential role for macrophage migration inhibitory factor (MIF) in angiogenesis and the growth of a murine lymphoma. Mol Med 1999, 5:181–191
42. Shimizu T, Abe R, Nakamura H, Ohkawara A, Suzuki M, Nishihira J: High expression of macrophage migration inhibitory factor in human melanoma cells and its role in tumor cell growth and angiogenesis. Biochem Biophys Res Commun 1999, 264:751–758